Title
NOTE ON THE Pt AND Hg MASS-197 ISOMERS

Authors
Haverfield, A. J.
Easterday, H.T.
Hollander, J.M.

Publication Date
1964-08-01

UCRL-11607

University of California

Ernest O. Lawrence Radiation Laboratory

NOTE ON THE Pt AND Hg MASS-197 ISOMERS

Berkeley, California

DISCLAIMER

Nuclear
Phys.

UCRL-11607

UNIVERSITY OF CALIFORNIA

Lawrence Radiation Laboratory
Berkeley, California

AEC Contract No. W-7405-eng-48

NOTE ON THE Pt AND Hg MASS-197 ISOMERS

A. J. Haverfield, H. T. Easterday, and J. M. Hollander

August 1964

NOTE ON THE Pt AND Hg MASS-197 ISOMERS*

A. J. Haverfield, H. T. Easterday,† and J. M. Hollander

Lawrence Radiation Laboratory
University of California
Berkeley, California

August 1964

Abstract

The decays of Pt^{197}, Pt^{197m}, Hg^{197} and Hg^{197m} into the levels of $_{79}Au^{197}$ have been examined with use of semiconductor detector spectrometers. Gamma-ray spectra were recorded with lithium drifted germanium detectors, and internal conversion coefficients were measured with an electron-gamma spectrometer employing both silicon and germanium detectors.

These conversion coefficients were determined: the 191-keV transition in Au^{197} following Pt^{197} decay, $\epsilon_K = 0.69 \pm 0.07$, $K/L = 5.2 \pm 0.6$; the 346-keV transition in Pt^{197m}, $\epsilon_K = 3.9 \pm 0.4$, $K/L = 1.8 \pm 0.2$. The 191-keV transition is interpreted as having multipolarity M1 + (~28%) E2, and the 346-keV is an M4.

Details of the decay schemes are discussed. From the observed decay patterns of Pt^{197} and Pt^{197m}, spin assignments 1/2- and 13/2+ are made for these isomers, respectively. The spin of the 268-keV level in Au^{197} is interpreted as 3/2+, consistent with the "core-excitation" interpretation of these levels by Braunstein and de Shalit.

The reported existence of a level in Au^{197} at 155 keV was not confirmed, and a reported weak 407-keV radiation from the decay of Hg^{197m} was not observed.

The absolute transition probability of the 202 keV E2 radiation connecting the 279 keV (5/2+) and 77 keV (1/2+) states is discussed, within the framework of the de Shalit model and also that of Kisslinger and Sorensen.

---

*This work was done under the auspices of the U. S. Atomic Energy Commission.

†On leave from Oregon State University, Corvalis, Oregon.

1. Introduction

The low-lying energy levels of $_{79}Au^{197}$ are well-known as the result of studies of the decays of 18-h $_{78}Pt^{197}$, 65-h $_{80}Hg^{197}$, 24-h Hg^{197m}, and also from studies of particle inelastic scattering on Au^{197}. The six known levels in Au^{197} below 600 keV have been discussed by Braunstein and de Shalit[1]) in terms of two intrinsic single proton states, $d_{3/2}$ (ground) and $h_{11/2}$ (409 keV) plus a quadruplet (1/2, 3/2, 5/2, 7/2) arising from the coupling of a 2+ core-excitation with the $d_{3/2}$ proton. This situation is represented in fig. 1.

The experiments described herein were motivated by the following considerations: 1) as pointed out by Artna[2]), doubt has been cast on the assignment of spin 3/2 to the 268 keV level as a result of the recent measurements by Joshi et al.[3]) of the internal conversion coefficient of the 191-keV transition. The value obtained by these workers, 2.0 ± 0.5, is considerably higher than the theoretical value[4]) for a pure M1 transition, 0.79, and suggests that the 191-keV transition has E0 admixture and therefore that the 268-keV state has spin 1/2 rather than 3/2 as previously thought. 2) A recent paper by Griesacker and Roy[5]), reporting the results of beta-gamma and gamma-gamma coincidence experiments on neutron irradiated Pt^{196} (enriched), has suggested a more complicated decay scheme for Pt^{197} and Pt^{197m} than had previously been accepted, and also a new level in Au^{197} at 155 keV was reported. 3) The multipolarity of the iosmeric transition in Pt^{197m} had not been definitely established.

Accordingly, we have studied the decays of Pt^{197}, Pt^{197m}, Hg^{197}, and Hg^{197m} in an effort to shed further light on these questions. Briefly, we have (1) found the 191-keV transition to be an M1-E2, not an M1-E0, mixture; (2) established the multipolarity of the 346-keV transition in Pt^{197m} to be M4; and (3) shown that the spin of Pt^{197} is 1/2. However, we do not confirm the reported[5]) existence of a level in Au^{197} at 155 keV.

2. Experimental Procedure and Instrumentation

Samples of 18-h Pt^{197} and 97-minute Pt^{197m} were prepared by the neutron irradiation of isotopically enriched Pt^{196}* in the G. E. reactor at Vallecitos, California. An average thermal flux of 1.8×10^{13} $n/cm^2 \cdot sec$ was used, with a slow/fast neutron ratio of 7.3/1. Chemical purification of the platinum from gold (principally Au^{199}) was done by extraction of the gold into amyl acetate, following dissolution of the sample in aqua regia. A portion of the Pt fraction was liquid-deposited on to a gold-coated mylar source backing for electron and gamma counting; the Au fraction was examined only in solution for the gamma spectrum. Samples of 24-hour Hg^{197} and 65-hour Hg^{197m} were prepared by irradiation of gold metal (Au^{197}) with 15-MeV deuterons in the L.R.L. 88-inch cyclotron. Carrier-free Hg sources were obtained by distillation of mercury from the gold target at ~ 800° C in a quartz vessel on to a water-cooled gold disc. A 2-mm circular collimator defined the area of the Hg deposit.

Gamma ray spectra were observed with a liquid-nitrogen-cooled lithium-drifted germanium (Ge(Li)) detector of dimensions 4 cm^2 × 7 mm deep, coupled to a low-noise preamplifier-amplifier system designed by Goulding and Landis[6,7]. The detectors and the associated electronics were all fabricated at this Laboratory[8]. Internal conversion coefficients were measured with an electron-gamma spectrometer, designed for this purpose, which utilizes Si(Li) and Ge(Li) detectors for quantitative measurement of the electron and gamma-ray spectra, respectively[9]. Dimensions of the detectors in this apparatus are: silicon, 1 cm^2 × 3 mm; germanium, 4 cm^2 × 5 mm.

---

*Obtained from Stable Isotopes Division, Oak Ridge National Laboratory, Oak Ridge, Tennessee. Isotopic analysis of this material was: $Pt^{190} < 0.05\%$, $Pt^{192} < 0.05\%$, Pt^{194} 6.57%, Pt^{195} 26.18%, Pt^{196} 65.55%, Pt^{198} 1.70%.

The performance of the gamma-ray spectrometer is illustrated in fig. 2. In this spectrum, a half-width of 2.3 keV is obtained for the 122- and 136-keV photons of Co^{57}. Figure 3 shows the electron and gamma spectra of the 279-keV transition in Hg^{203}, recorded with the conversion-coefficient spectrometer. In this spectrum, resolution of the electron side of 4.2 keV, and that of the gamma-ray side is 4.6 keV.

3. Gamma Spectra—Pt^{197} and Pt^{197m}

Subsequent to a 4-hour irradiation of enriched Pt^{196}, a series of gamma spectra of the Pt-fraction was recorded with the 2 cm^2 Ge(Li) detector. The multi-channel analyzer was programmed to record the spectrum for 30-minutes, print out, and re-cycle. This was continued for a period of 9 hours. The first 30 minute spectrum, taken about 3 hours after the end of irradiation, is shown in fig. 4a. Figure 4b shows a spectrum, started approximately 12 hours after the end of irradiation, and run for 15 hours. In fig. 5, the intensities of the major peaks are plotted as a function of time. The known half-lives of Pt^{197} (18 hr) and Pt^{197m} (~ 97 min) are clearly distinguished, with no evidence of compound decay. The 279- and 346-keV photons arise from Pt^{197m} decay; the 77-, 191- and 268-keV photons arise from Pt^{197} (g.s.) decay.

Other, weaker, photons observed in the early spectra include the 246- and 317-keV photons of 30-minute Pt^{199} (produced from Pt^{198} in the target material) and the 99- and 130-keV photons of Pt^{195m} (produced from Pt^{194}). In the later spectra, the 158- and 208-keV photons of Au^{199} and the 293- and 328-keV photons of Ir^{194} are observed in low intensity from these impurities.

The intense 155-keV gamma ray reported by Griesacker and Roy[5] as arising from the decays of Pt^{197} and Pt^{197m} is not observed. From the spectrum

of fig. 4a, an upper limit to its intensity can be set as 0.5% of the 191-keV photon of Pt^{197} or as 20% of the 279-keV photon of Pt^{197m}. A similar situation applies with the 202-keV gamma ray reported by these authors. Our $Pt^{197 + 197m}$ spectrum shows that the intensity of the 202-keV photon is less than ~ 5% of the 279-keV photon in Pt^{197m} decay, whereas the spectrum of Griesacker and Roy indicates that the 202-keV gamma is stronger than the 279-keV gamma. It is possible that the 155- and 202-keV gammas reported by Griesacker and Roy were in reality due to the prominent 158- and 208-keV gammas of Au^{199}, which would have been an impurity in their source since a radio-chemical separation was not performed in their experiments. In fig. 6 we show for comparison the gamma spectrum of the gold chemical fraction from our "Pt^{196}" + n irradiation; the prominent radiations of Au^{199} are obvious.

A very weak 358-keV gamma-ray of unknown origin was also seen in our early gamma spectra; it decays with a ≈ 50 minute half-life.

Table 1 summarizes the gamma-ray data on Pt^{197} and Pt^{197m}. Included in this table is the 53-keV E2 transition of Pt^{197m} found by Sehgal and Emery[10]). This transition was not observed in our photon spectrum because of its large conversion coefficient ($e/\gamma \sim 100$).

4. Gamma Spectra—Hg^{197} and Hg^{197m}

A series of timed gamma spectra was recorded of the purified Hg fraction from the Au + d bombardment, in a manner similar to that of the Pt^{197} experiments. Figure 7 is a reproduction of the $Hg^{197 + 197m}$ spectrum. All photon lines seen in this spectrum decayed with single periods (the 22-hour half-life of Hg^{197m} or the 66-hour half-life of Hg^{197}) except for the weak 263-keV line, whose assignment is uncertain. Figure 8 shows the decay curves

of the various gamma-ray lines, and Table 2 contains a summary of the photon intensity data on Hg^{197} and Hg^{197m}.

It is interesting to note that, in spite of many previous investigations of these iosmers, the 268-keV gamma had not been reported in the decay of 66-hour Hg^{197} [11]. The Ge(Li) spectrum of fig. 7 clearly shows its presence, and the decay curves of fig. 8 confirm its 66-hour half-life. In the decay of 22-hour Hg^{197m}, the weak 202-keV gamma-ray had previously been unreported.

A few words may be stated about the 407-keV M4 crossover gamma ray in Au^{197} that has been reported[13]. We find no evidence for this gamma ray either in Hg^{197m} or Pt^{197m} decay, and our data allow the following upper limits of its intensity to be set:

from Pt^{197m} decay: $I(409) / I(279) < 0.04$;

from Hg^{197m} decay: $I(409) / I(279) < 0.001$.

5. Internal Conversion Coefficients

Measurements were made of the K- and L- internal conversion coefficients of the 191-keV transition of Pt^{197} decay and of the 346-keV transition of Pt^{197m} decay. The electron-gamma semiconductor spectrometer used for these measurements has been described elsewhere[9]. Essentially, this device contains Si(Li) and Ge(Li) detectors for observation of the electron and gamma spectra, respectively, and the system is calibrated for quantitative measurements by use of several well-known conversion coefficients.

The conversion coefficient is determined from the following relationship:

$$\epsilon = \frac{A_e}{A_\gamma} \cdot \frac{\eta_\gamma(E_\gamma)}{\eta_e(E_e)}$$

where A_e is the area under the conversion electron peak.

A_γ is the area under the corresponding gamma-ray peak.

$\eta_\gamma(E_\gamma)/\eta_e(E_e)$ is the ratio of detector efficiencies of the Ge and Si detectors for the relevant photon and electron energies. The normalized efficiency curves are given in reference 9.

The five previously reported measurements of the K- conversion coefficient of the 191-keV transition in Au^{197} (summarized in Table 3) show a spread from 0.65 to 2.5. The theoretical K-conversion coefficient of Sliv[4]) for an M1 transition of this energy is 0.95, and that for an E2 transition is 0.185. According to the interpretation of the Au^{197} levels as represented in fig. 1, the 191-keV transition can be M1 or an M1-E2 mixture. Thus, it is significant if the true value of this conversion coefficient is established to be higher than 0.95 because this would imply E0 admixture in the 191-keV transition, and thus the spin of the 268-keV level would have to be assigned as 1/2 + in contradiction to the model of Braunstein and de Shalit (fig. 1).

The appropriate portions of our $Pt^{197 + 197m}$ electron and gamma spectra are shown in figs. 9a and 9b. From these and similar spectra the data of Table 4 were obtained. Comparison of the experimental conversion coefficient, 0.69 ± 0.07, with the theoretical values of Sliv yields the result that the 191-keV transition is an M1-E2 mixture with 33 ± 9% E2 admixture. The K/L ratio, 5.2 ± 0.6, indicates a 22 ± 11% E2 admixture. This result is consistent with the assignment of the 268-keV level as 3/2+ and thus with the core-excitation interpretation of the Au^{197} levels as given by Braunstein and de Shalit[1]).

In Table 5 are given the data for the 346-keV transition of Pt^{197m} decay. The experimental values, $\epsilon_K = 3.9 \pm 0.4$ and $K/L = 1.8 \pm 0.2$, clearly establish the multipolarity of this transition as M4 since the theoretical M4 values[4]) are $\beta_k(M4) = 4.2$, $K/L = 1.75$.

6. Beta Decay of the Mass-197 Isobars; Spin Assignment of Pt^{197}

It is of interest to compare the decay properties of the isomers of Pt^{197} with those of the Hg^{197} isomers. The Hg^{197} ground-state, with a measured spin 1/2[16]), and $p_{1/2}$ assignment, decays to the 77-keV level (98%, log ft = 5.9) and to the 268-keV level (2%, log ft = 7.0)[11]). From our experimental upper limit on the intensity of the 279-keV gamma ray in Hg^{197} decay (see Table 2), we can set an upper limit for electron-capture to the 279-keV state as 0.022%. This corresponds to a log ft lower-limit of 8.9, which is consistent with the accepted interpretation of this transition as a "$\Delta I = 2$, yes" type.

The situation with Pt^{197} has not been clear. The Pt^{197} ground state has variously been assigned spin 1/2 or 3/2. Most recently, the value 3/2 has been adopted, from an analysis of existing data[11]). This choice was based on the reported observation of a weak 279-keV photon from Pt^{197} decay and its interpretation as arising from a weak beta branch of Pt^{197} to the 279-keV (5/2+) level[15]). Our data on Pt^{197} support neither this observation nor its interpretation. The radiation from Pt^{197} which had been reported[15]) as "279 keV" is seen from our gamma spectra actually to be the 268-keV crossover gamma-ray. The 279-keV gamma-ray that is observed in our spectra decays with the 97-minute half-life of Pt^{197m}, not with the 18-hour half-life of Pt^{197}, and it is possible to set a quite small upper limit on its intensity in Pt^{197} decay (see Table 1). From this upper limit we calculate an upper limit for beta decay of Pt^{197} to the 279-keV level in Au^{197} as 0.013%, which corresponds to a log ft value $\geq$ 9.7. This log ft limit is consistent with the interpretation of the beta decay branch to the 279-keV level as a "$\Delta I = 2$, yes" type (same as the corresponding Hg^{197} transition). Therefore it appears that the correct assignment for the Pt^{197} ground-state is 1/2-, as it is for Hg^{197}.

With the $p_{1/2}$ assignment for the Pt^{197} ground-state and the known multipolarities of the 53 keV (E2) and the 346-keV (M4) cascade transitions, the isomeric state is assigned as $13/2+$ $(i_{13/2})$.

It is possible from the observed gamma-ray intensities to calculate the beta decay branching of Pt^{197m} with use of the following relationship.

$$\% \beta^- = \frac{1}{1 + \frac{I_{346\gamma}(1 + \epsilon_{346})}{I_{279\gamma}(1 + \epsilon_{279})}} \times 100$$

$$= \frac{1}{1 + \frac{100(1 + 6.7)}{21(1 + 0.3)}} \times 100$$

$$= 3.4 \pm 1\%$$

The conversion coefficient of the 346-keV transition used for this calculation is essentially our measured value (corrected for M, N...conversion) and that used for the 279-keV transition is an estimate based on the assumption of an M1-E2 transition with ~25% E2 admixture.

A similar calculation for Hg^{197m}, made with use of the relative intensities of the 164-keV and 279-keV gammas and the theoretical M4 conversion coefficient for the 164-keV transition, yields the result that the electron capture branching of Hg^{197m} occurs in 6.8% of the decays. An independent calculation using the relative intensities of the 130-keV and 279-keV gammas yields the value 6.5%.

7. Discussion

Figure 10 shows the decay schemes of the Pt^{197} and Hg^{197} isomers. Not shown in this figure is the 7/2+ level of Au^{197} at 548 keV, since this state is not populated by their decays.

The present data have suggested some simplifications in the mass 197 level scheme. In particular, the ground-state spin and parity assignment of $_{78}Pt^{197}$ appears to be the same as that of $_{80}Hg^{197}$ (1/2-) and the two corresponding isomeric states also have the same assignment (13/2+) and decay patterns.

Fairly well established is the existence of the quadruplet of excited states in Au^{197} with spins 1/2, 3/2, 5/2, and 7/2 (even parity). As mentioned earlier, Braunstein and de Shalit[1]) have proposed the simple model of a one-phonon excitation coupled to the $d_{3/2}$ particle state to describe the predominant features of this quadruplet. The model is able to account for the small magnetic moment of the 77 keV (1/2+) state and also to correlate the observed transition probabilities from the one-phonon states to the ground state.

One additional piece of information obtained in the study reported here derives from the observation of the 202 keV radiation that connects the 279 and 77 keV states. The measured relative photon intensity of this transition, which must be an E2 if the state assignments are correct, allows one to calculate the absolute photon transition probability. The resulting value may be compared with predictions of specific nuclear models.

From the measured photon intensities (Table 2) together with the known half-life of the 279-keV state (1.6×10^{-11} sec) and an estimated conversion coefficient of the 279 keV transition (0.3), we calculate the absolute transition probability of the 202 keV E2 photon to be 4.9×10^{8} sec^{-1}. The single proton transition rate, calculated from the Moszkowski formula with $a = 1.2 \times 10^{-13}$ cm instead of 1.45×10^{-13} cm is 0.29×10^{8} sec^{-1}. Thus the observed E2 transition

probability between the 5/2+ and 1/2+ states of the "quadruplet" is more than an order of magnitude greater than the single particle rate. On the other hand, the results of a preliminary calculation of B(E2) by Thankappan and Rasmussen[17]) made with use of the wave functions given by de Shalit[18]) for the nearly pure $d_{3/2}$ + phonon states indicate that this E2 transition probability would be about one-third the single-particle value. Thus there appears to be a discrepancy between our experimental result and the de Shalit wave-functions.

In a generalized theoretical treatment of the energy levels and moments of spherical nuclei, Kisslinger and Sorensen[19]) have included a description of the levels of $_{79}Au^{197}$. In their model, the 1/2+ level at 77 keV is composed of about 92% $s_{1/2}$, 3% $d_{5/2}$ + phonon, and 4% $d_{3/2}$ + phonon, and the 5/2+ level at 279 keV is made up of about 2% $d_{5/2}$, 0.1% $d_{5/2}$ + phonon, 74% $d_{3/2}$ + phonon, and 8% $s_{1/2}$ + phonon. It is likely that this description could better account for the large observed $B(E2)_{5/2 \rightarrow 1/2}$ than the simpler "core-excitation" model because here there is a contribution to the E2 transition rate from $5/2_{(s_{1/2}+ \text{ phonon})} \rightarrow 1/2_{(s_{1/2})}$, which would be expected to be a fast transition.

It is interesting to point out that both the Kisslinger and Sorensen model and the de Shalit model predict magnetic moments for the 77 keV 1/2+ level that are small, and close to the experimental value. Thus in this case it appears that the E2 transition probability may provide a more sensitive test of the two models than the magnetic moment.

Acknowledgments

We acknowledge with gratitude the essential contribution of F. S. Goulding and his colleagues in the development of the semi-conductor counting systems. In this regard, thanks are especially due C. A. Crayne, W. L. Hansen, B. Jarret, G. W. Kilian, D. A. Landis, and C. E. Miner. We are grateful also for the technical assistance rendered by C. J. Butler and J. A. Harris.

Thanks are due Professor J. O. Rasmussen for several enlightening discussions.

References

1) A. Braunstein and A. de Shalit, Phys. Letters 1 (1962) 264

2) A. Artna, private communication (Jan. 1963)

3) M. C. Joshi and B. V. Thosar, Proc. Intern. Conf. Nucl. Structure, Kingston, Canada, D. A. Bromley and E. V. Vogt, Ed. Univ. of Toronto Press (1960) p. 623

4) L. A. Sliv and I. M. Band, Coefficients of internal conversion of gamma radiation (USSR Academy of Sciences, Moscow-Leningrad, 1956) Part I: K Shell, Part II: L Shell

5) P. B. Griesacker and R. R. Roy, Nucl. Phys. 50 (1964) 41

6) F. S. Goulding and D. Landis, Proceedings of Conference "Instrumentation Techniques in Nuclear Pulse Analysis", Monterey, April 1963, N.A.S.-N.R.C. publication 1184

7) F. S. Goulding, UCRL-11302 (Feb. 1964)

8) F. S. Goulding and W. L. Hansen, UCRL-11261 (Feb. 1964)

9) H. T. Easterday, A. J. Haverfield and J. M. Hollander, Nucl. Instr. and Methods (to be published)

10) M. Sehgal and G. T. Emery, private communication (July 1964)

11) See, e.g., Nuclear Data Sheets, published by Nuclear Data Group, Oak Ridge National Laboratory, Oak Ridge, Tennessee

12) L. Feuvrais, Ann. Phys. 5 (1960) 181

13) R. Joly, J. Brunner, J. Halter and O. Huber, Helv. Phys. Acta 28 (1955) 403

14) O. Huber, F. Humbel, H. Schneider, A. de Shalit and W. Zunti, Helv. Phys. Acta 24 (1951) 127

15) V. R. Potnis, C. E. Mandeville and J. S. Berlew, Phys. Rev. 101 (1956) 753

16) W. G. Procter and F. C. Yu, Phys. Rev. 81 (1951) 20

17) V. K. Thankappan and J. O. Rasmussen, unpublished results (July 1964)

18) A. de Shalit, Phys. Rev. 122 (1961) 1530

19) L. S. Kisslinger and R. A. Sorensen, Rev. Mod. Phys. 35 (1963) 853

Table 1

Photons of Pt^{197} and Pt^{197m} decay

	Energy (keV)	Relative Intensity
Pt^{197}	77	33 ± 3
	191.4	100
	268	7 ± 1
	279 (not seen)	< 0.2
Pt^{197m}	52.95[a]	———
	(130)[b]	———
	202	≤ 1
	279	21 ± 2
	346	100

[a] L-subshell conversion electrons observed by Sehgal and Emery[10].

[b] Photons of this E3 transition not seen because of large conversion coefficient ($e/\gamma \sim 25$).

Table 2

Photons of Hg^{197} and Hg^{197m} decay

	Energy (keV)	Relative Intensity
Hg^{197}	77	———
	191	100
	268	7.6 ± 0.7
	279 (not seen)	< 2
Hg^{197m}	134	100
	165	0.95 ± 0.1
	202	0.23 ± 0.03
	279	15.7 ± 1

Table 3

Reported values of the K conversion coefficient of the 191-keV transition in Au^{197}

ϵ_K	Reference
0.65 ± 0.15	12
0.90 ± 0.10	13
≈ 1.7	14
2.0 ± 0.5	3
2.5	15

Table 4. K-conversion coefficient and K/L conversion ratio of 191-keV transition in Au^{197}

Run	A_K/A_γ	$\epsilon = \frac{A_K}{A_\gamma} \cdot \frac{\eta_\gamma}{\eta_e}$ [a]	A_K/A_L	$K/L = \frac{A_K}{A_L} \cdot \frac{\eta_L}{\eta_K}$ [a]
1	1.141	0.705	5.87	4.95
2	1.025	0.633	6.72	5.67
3	1.200	0.742	4.78	4.04
4	1.149	0.710	6.23	5.26
5	1.088	0.672	6.54	5.52
6	1.051	0.649	6.68	5.64
7	1.104	0.682	----	----
		$\epsilon = 0.69 \pm 0.07$		$K/L = 5.2 \pm 0.6$

[a] Gamma-ray and electron efficiency values were taken from Figures 6 and 7 of Reference 9.

Table 5. K-conversion coefficient and K/L conversion ratio of 346-keV transition in Pt^{197m}

Run	A_K/A_γ	$\epsilon = \frac{A_K}{A_\gamma} \cdot \frac{\eta_\gamma}{\eta_K}$ [a]	A_K/A_L	$K/L = \frac{A_K}{A_L} \cdot \frac{\eta_L}{\eta_K}$ [a]
1	16.03	3.62	2.31	2.16
2	16.42	3.71	1.75	1.64
3	19.00	4.29	1.80	1.68
		3.9±0.4		1.8±0.2

[a] Gamma-ray and electron efficiency values were taken from Figures 6 and 7 of Reference 9.

Figure Captions

Figure 1. Energy levels of Au^{197} arranged according to the "core-excitation model of Braunstein and de Shalit (reference 1).

Figure 2. Co^{57} gamma-ray spectrum taken with 2 cm^2 × 7 mm deep Ge(Li) detector system.

Figure 3. Electron and gamma-ray lines of the 279-keV transition of Hg^{203} recorded with the conversion-coefficient spectrometer.

Figure 4a. Gamma-ray spectrum of sample containing principally Pt^{197} and Pt^{197m}, observed with 2 cm^2 × 7 mm deep Ge(Li) detector system. This spectrum, the first in a series of sixteen, was recorded 3 hours after end of irradiation

Figure 4b. Gamma spectrum No. 16 of series of fig. 4a, recorded 12 hours after end of irradiation

Figure 5. Decay curves of the various gamma-ray lines of Pt^{197} and Pt^{197m} shown in figs. 4a and 4b.

Figure 6. Gamma-ray spectrum of Au^{199}, observed with 2 cm^2 × 7 mm deep Ge(Li) detector system.

Figure 7. Gamma-ray spectrum of sample containing Hg^{197} + Hg^{197m}, observed with 2 cm^2 × 7 mm deep Ge(Li) detector system.

Figure 8. Decay curves of the various gamma-ray lines of Hg^{197} and Hg^{197m} shown in fig. 7.

Figure 9a. Electron spectrum of sample containing Pt^{197} and Pt^{197m}, recorded with 1 cm^2 × 3 mm deep Si(Li) detector of the conversion-coefficient spectrometer.

Figure 9b. Gamma-ray spectrum recorded simultaneously with the electron spectrum of fig. 9a by the 4 cm^2 × 5 mm deep Ge(Li) detector of the conversion-coefficient spectrometer.

Figure 10. Decay scheme of the A = 197 isomers of Hg and Pt. The 7/2+ level in Au^{197} at 548 keV is not shown in this figure.

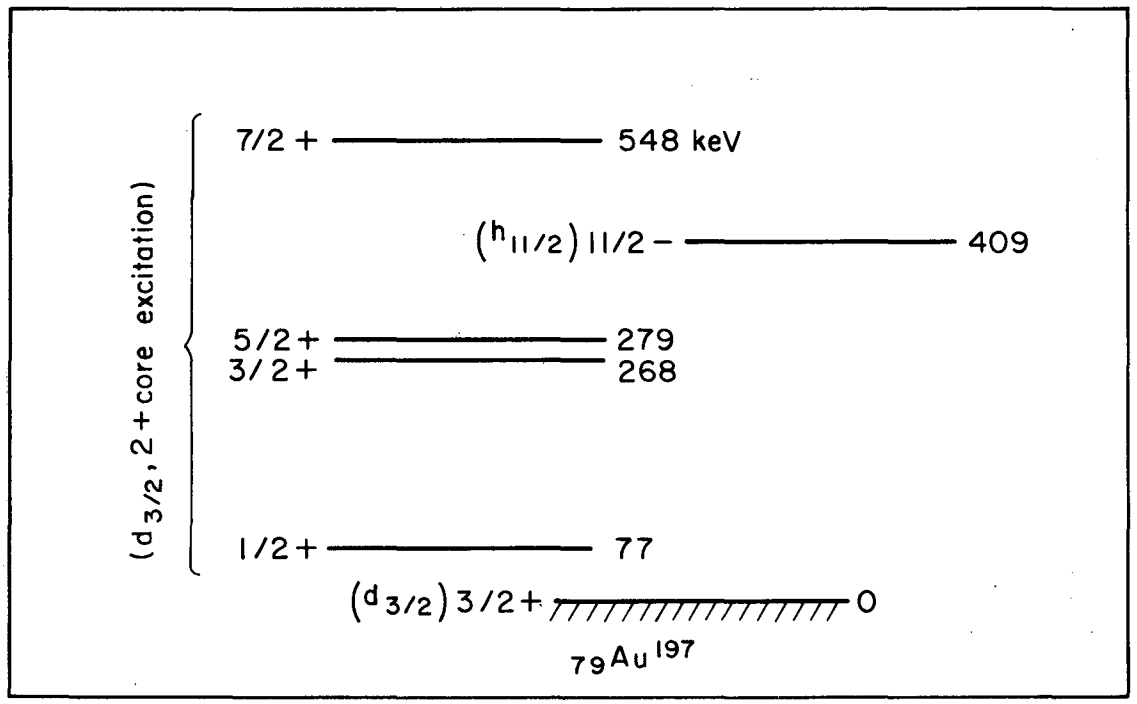

MUB-3888

Fig. 1

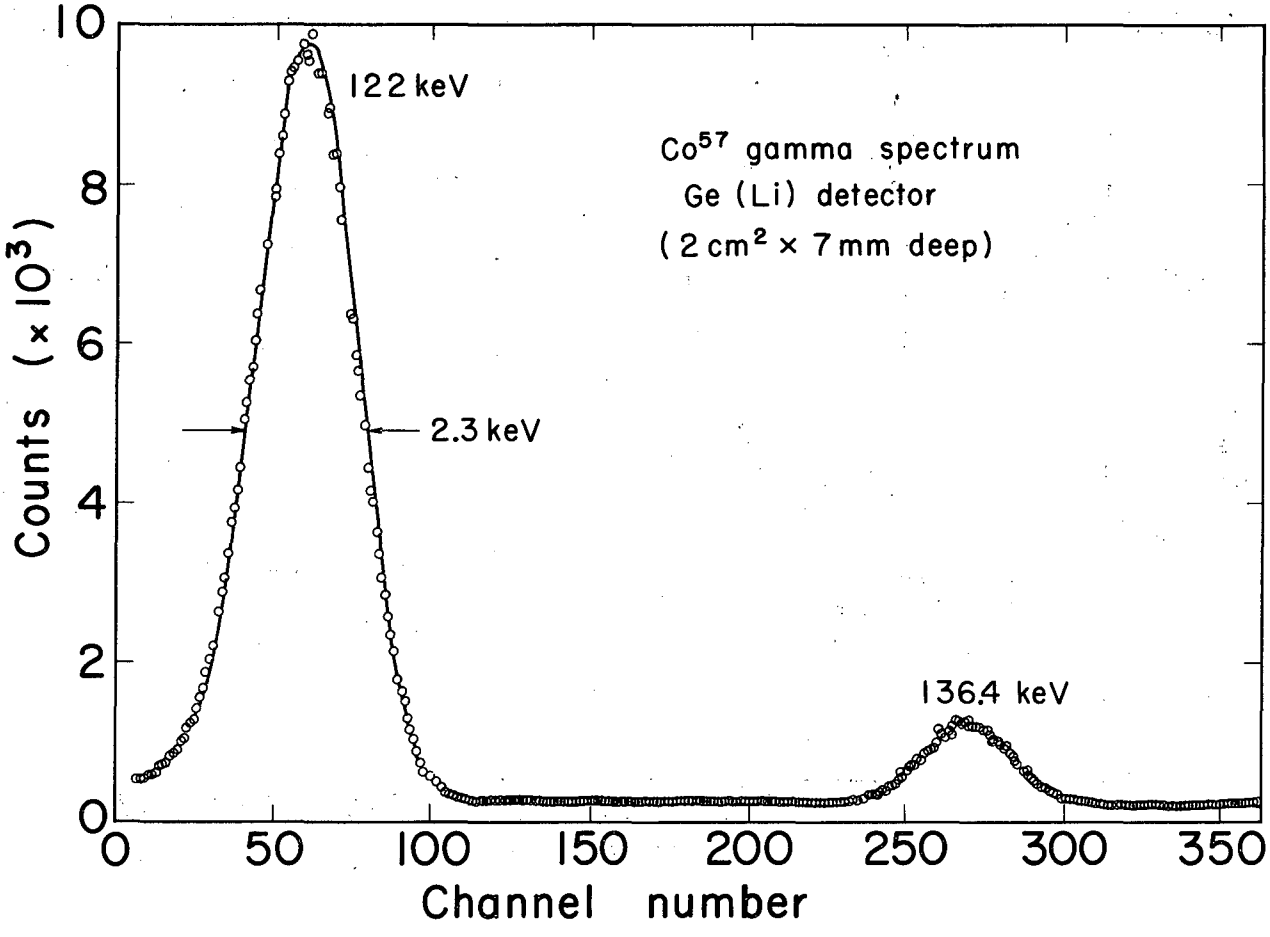
122 keV
Co57 gamma spectrum
Ge (Li) detector
(2 cm2 × 7 mm deep)
2.3 keV
136.4 keV
Counts (× 10³)
Channel number
0
2
4
6
8
10
0
50
100
150
200
250
300
350
MUB-3715

Fig. 2

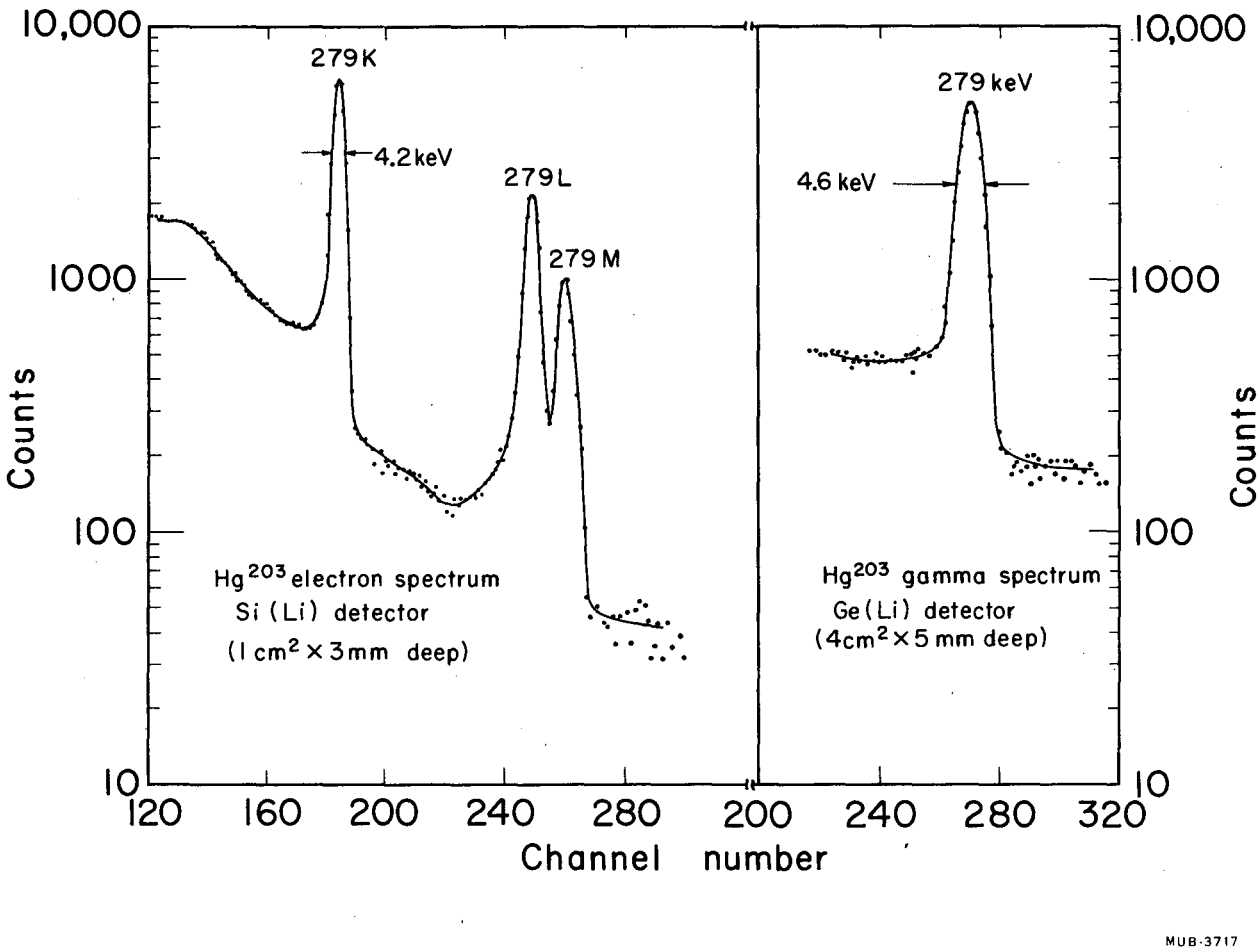
10,000
1000
100
10
Counts
279K
4.2keV
279L
279M
Hg203 electron spectrum
Si (Li) detector
(1 cm2 × 3mm deep)
279 keV
4.6 keV
Hg203 gamma spectrum
Ge(Li) detector
(4cm2 × 5 mm deep)
120
160
200
240
280
200
240
280
320
Channel number
MUB-3717

Fig. 3

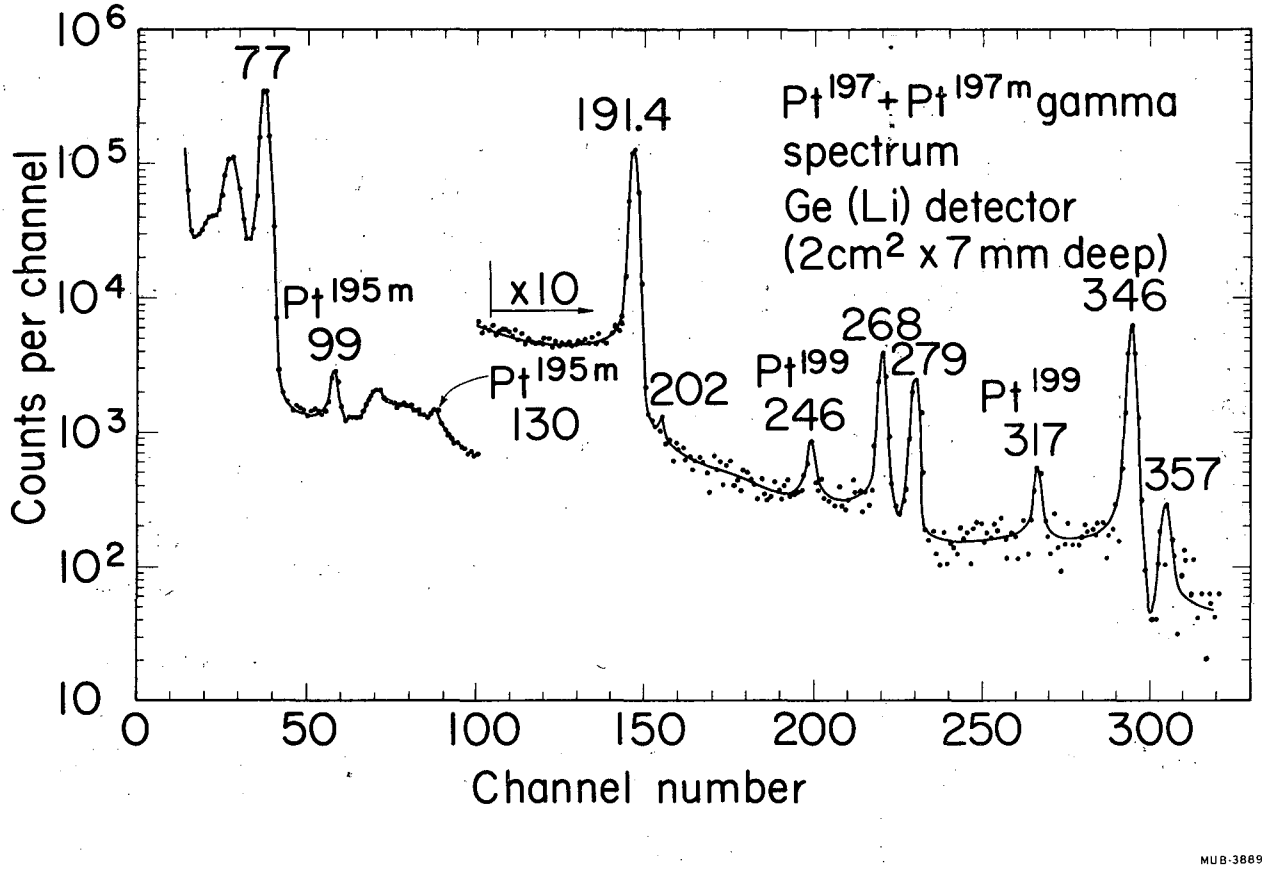
Counts per channel
Channel number
77
191.4
Pt197 + Pt197m gamma spectrum
Ge (Li) detector
(2cm² x 7 mm deep)
x10
Pt195m 99
Pt195m 130
202
Pt199 246
268
279
Pt199 317
346
357
MUB-3889

Fig. 4a

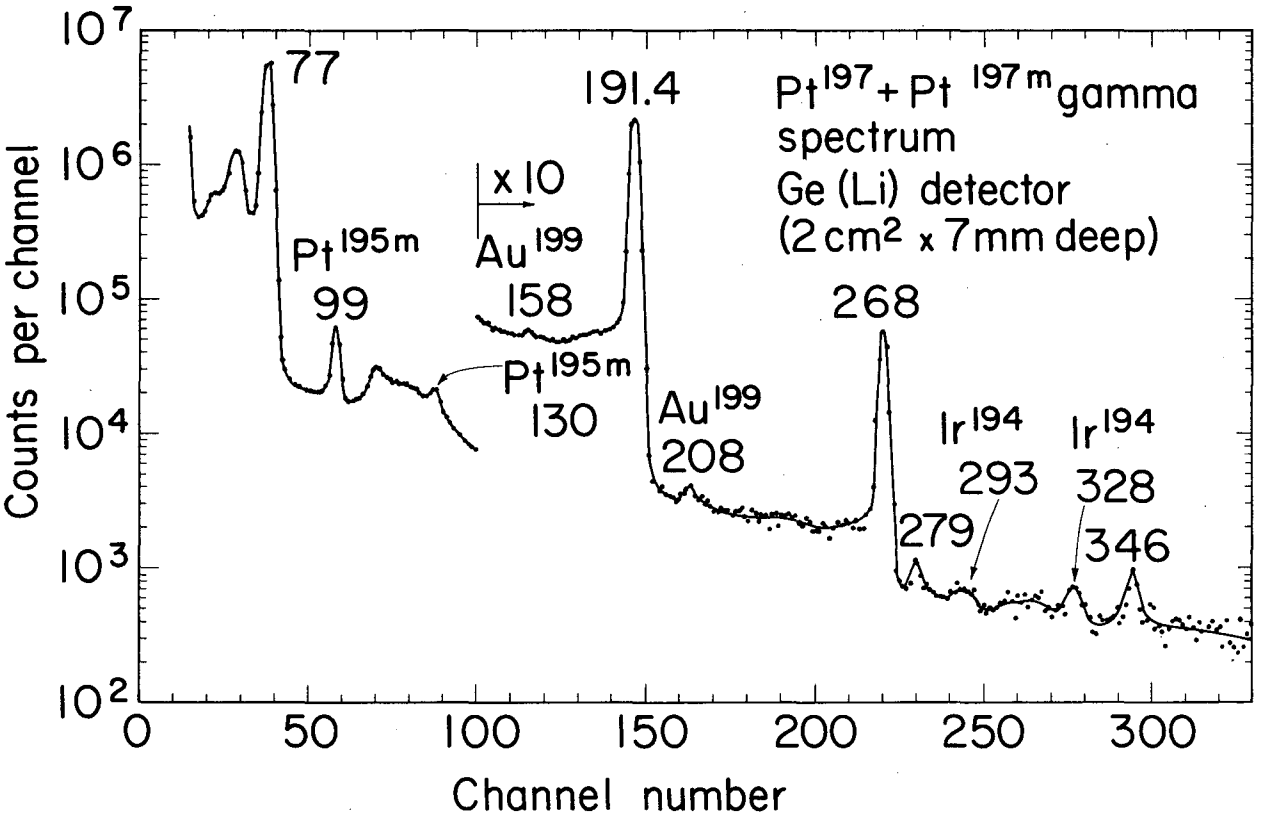
Counts per channel
Channel number
77
191.4
Pt197 + Pt 197m gamma spectrum
Ge (Li) detector
(2 cm2 x 7 mm deep)
x 10
Pt195m
99
Au199
158
Pt195m
130
Au199
208
268
Ir194
293
279
Ir194
328
346
MUB-3890

Fig. 4b

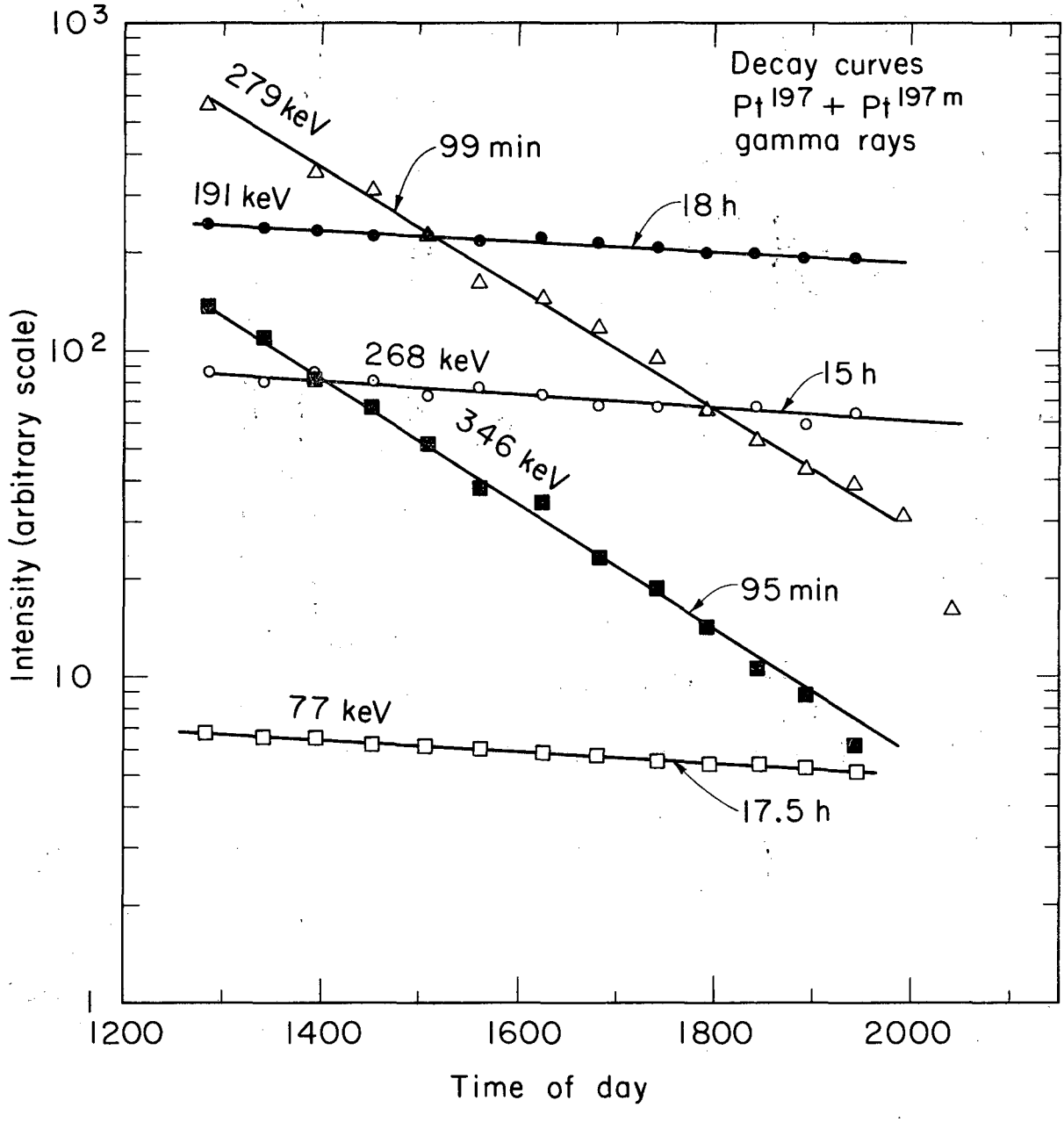
Decay curves
Pt 197 + Pt 197 m
gamma rays
279 keV
99 min
191 keV
18 h
268 keV
15 h
346 keV
95 min
77 keV
17.5 h
Intensity (arbitrary scale)
10 3
10 2
10
1
1200
1400
1600
1800
2000
Time of day
MUB-3891

Fig. 5

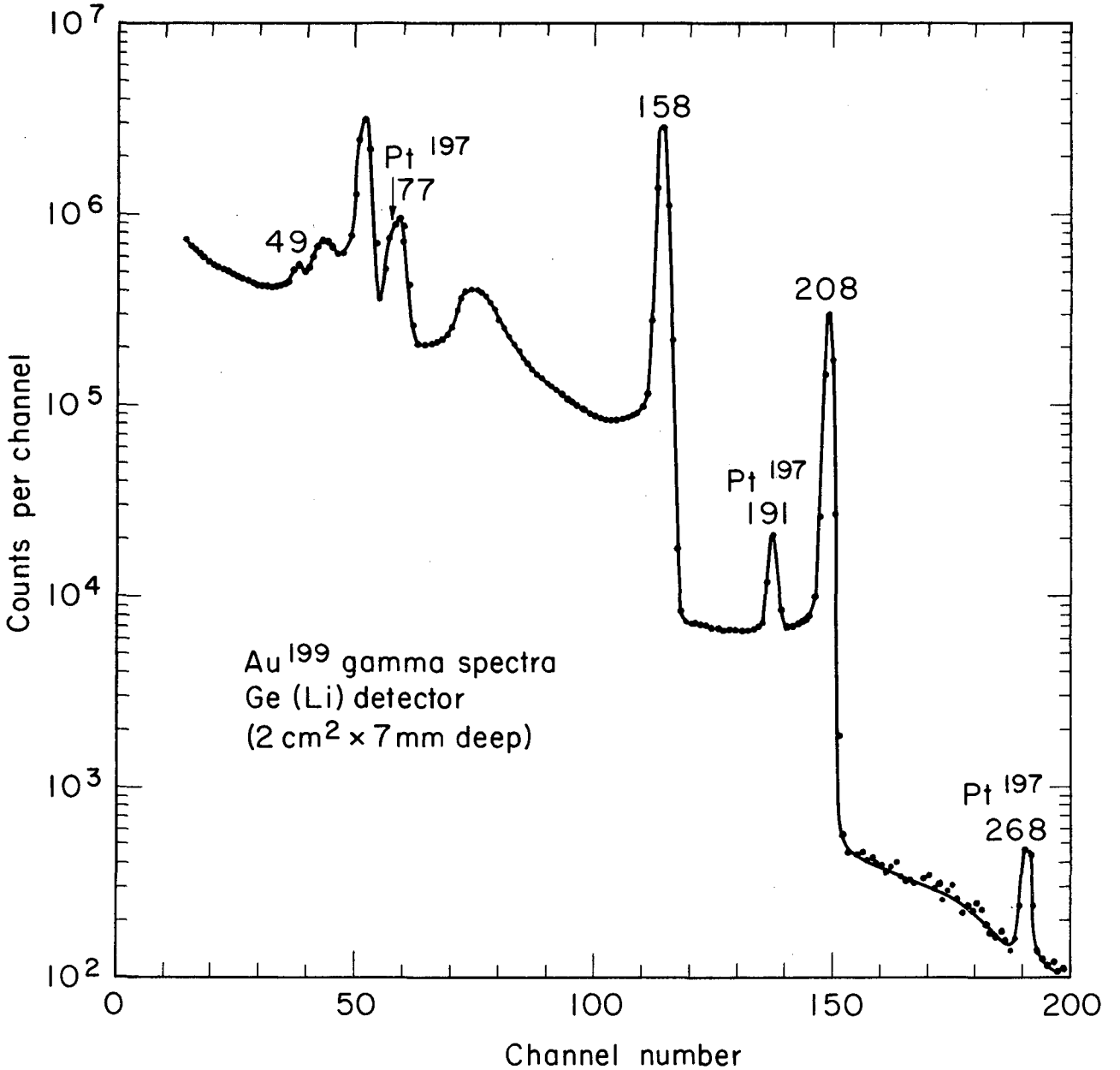
Counts per channel
Channel number
Au 199 gamma spectra
Ge (Li) detector
(2 cm2 x 7 mm deep)
158
Pt 197
77
49
208
Pt 197
191
Pt 197
268
MUB-3892

Fig. 6

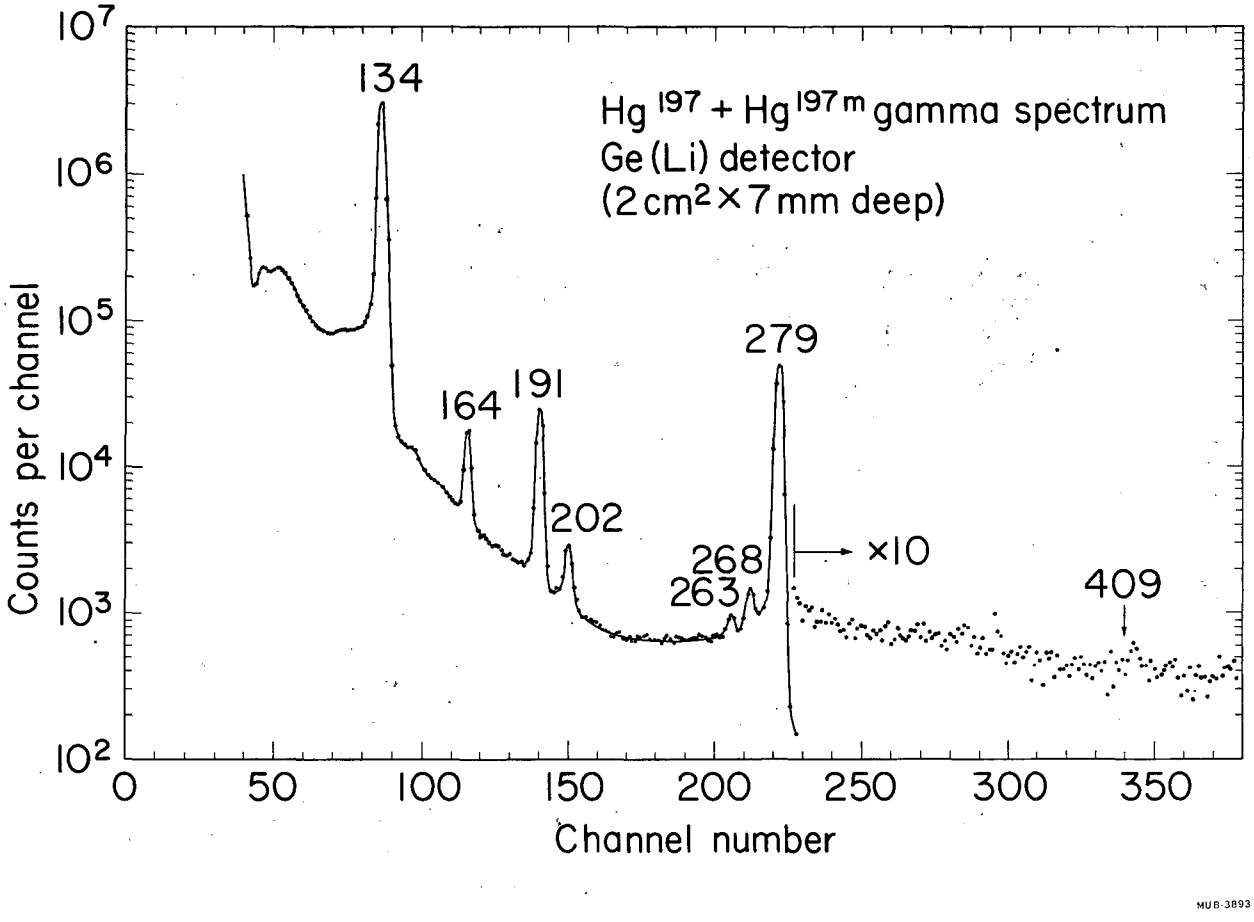
Hg 197 + Hg 197m gamma spectrum
Ge(Li) detector
(2 cm² × 7 mm deep)
134
164
191
202
263
268
279
×10
409
Counts per channel
Channel number
10⁷
10⁶
10⁵
10⁴
10³
10²
0
50
100
150
200
250
300
350
MUB-3893

Fig. 7

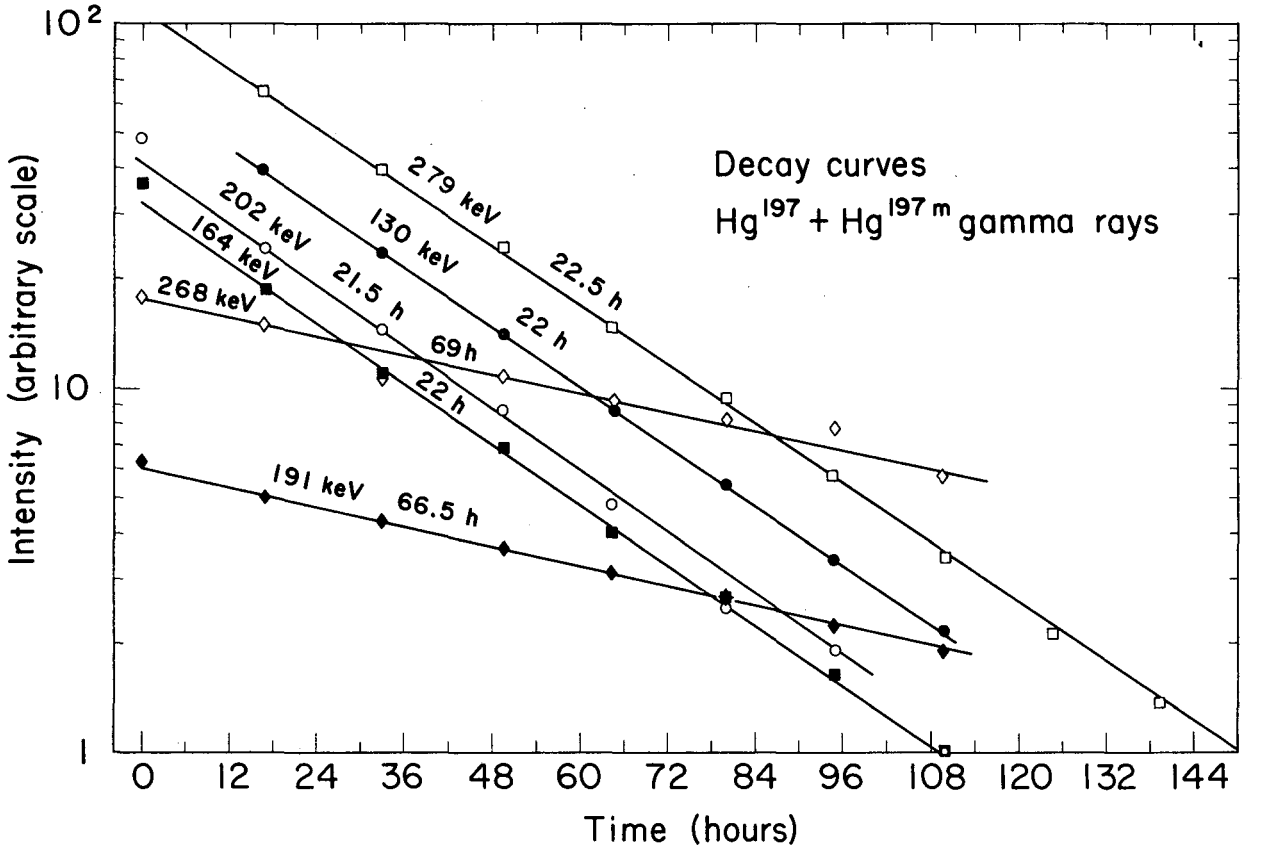
Decay curves
Hg197 + Hg197m gamma rays
279 keV
22.5 h
202 keV
130 keV
21.5 h
22 h
164 keV
69 h
268 keV
22 h
191 keV
66.5 h
Intensity (arbitrary scale)
10²
10
1
0
12
24
36
48
60
72
84
96
108
120
132
144
Time (hours)
MUB-3894

Fig. 8

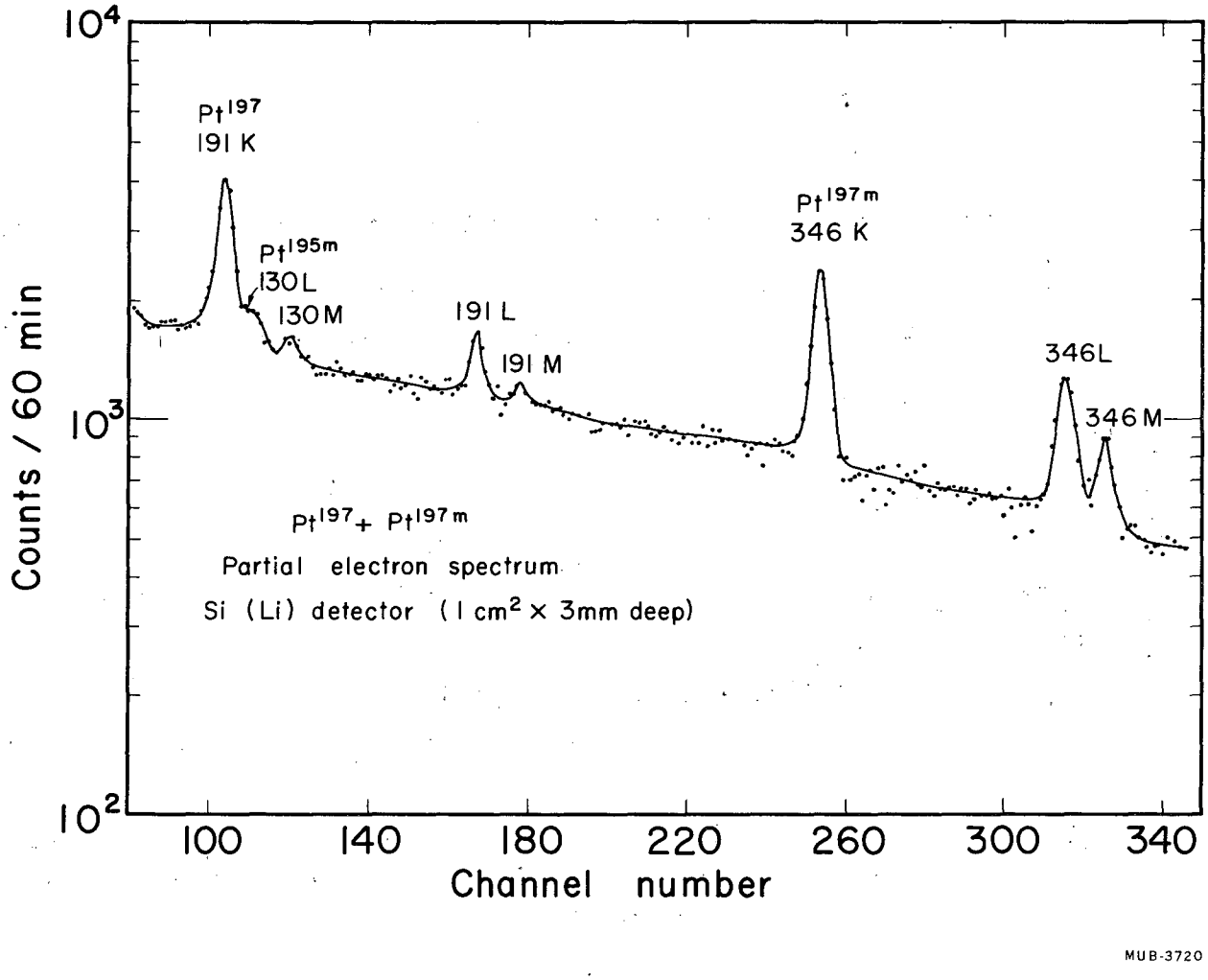
10^4
10^3
10^2
Counts / 60 min
Pt^{197}
191 K
Pt^{195m}
130 L
130 M
191 L
191 M
Pt^{197m}
346 K
346 L
346 M
Pt^{197} + Pt^{197m}
Partial electron spectrum
Si (Li) detector (1 cm^2 × 3mm deep)
100
140
180
220
260
300
340
Channel number
MUB-3720

Fig. 9a

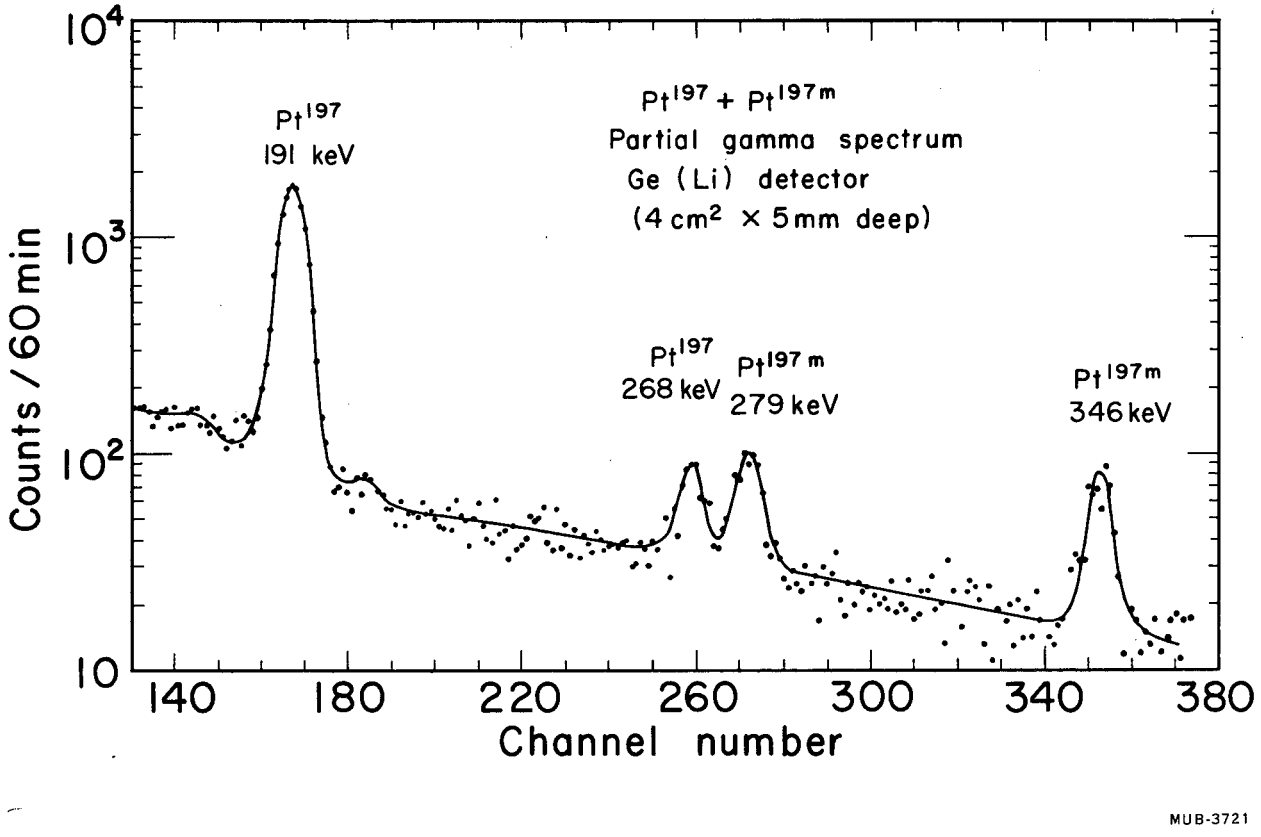
10^4
10^3
10^2
10
Counts / 60 min
Pt^{197}
191 keV
$Pt^{197} + Pt^{197m}$
Partial gamma spectrum
Ge (Li) detector
(4 cm² × 5mm deep)
Pt^{197}
268 keV
Pt^{197m}
279 keV
Pt^{197m}
346 keV
140
180
220
260
300
340
380
Channel number
MUB-3721

Fig. 9b

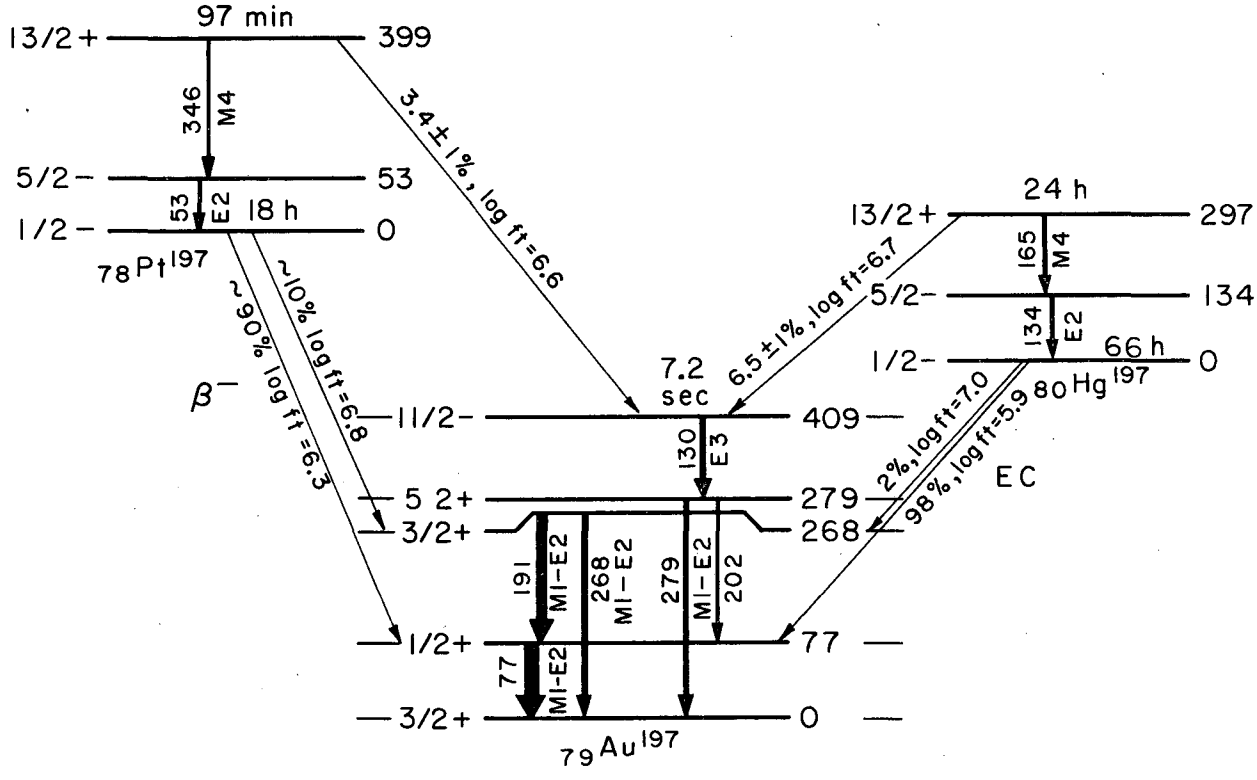

MUB-3895

Fig. 10